J Solid State Electrochem (2006) 10: 980–986
DOI 10.1007/s10008-005-0043-5

ORIGINAL PAPER

Mou Cheng Li · Jia Nian Shen

Photoelectrochemical oxidation behavior of organic substances on TiO_2 thin-film electrodes

Received: 17 May 2005 / Revised: 2 June 2005 / Accepted: 4 July 2005 / Published online: 10 August 2005

Abstract The photoelectrocatalytic oxidation characteristics of salicylic acid, formic acid and methanol on anodized nanoporous titanium dioxide (TiO_2) thin-films were investigated by using electrochemical impedance spectroscopy (EIS) and potentiodynamic polarization techniques. From dark to ultraviolet illumination, the open circuit potential (OCP) and film resistance of TiO_2 films decreased markedly. A general equivalent circuit model was proposed for the photoelectrochemical system anodic TiO_2 thin-film electrode/test solution. The photoelectrochemical oxidation process of the organic compounds showed similar impedance features at OCP and was controlled by the charge transfer step. According to the polarization curves of the base solution and organic solutions, the kinetic rate curves for the photoelectrocatalytic oxidation of pure organic species were obtained as a function of the potential bias. One photooxidation peak was first observed at a bias potential of ca. 0.26 V for these species with low concentrations.

Keywords Titanium dioxide film · Photoelectrocatalytic oxidation · Potential bias · EIS · Photocatalysis

Introduction

The photocatalytic oxidation effect of titanium dioxide (TiO_2) has been extensively investigated for removing organic pollutants in the recent 10 years [1–3]. This photocatalytic technique is regarded as a very promising method to solve many serious environmental problems, especially to remove trace organic species undecomposable by the conventional water treatments. There are some photocatalytic systems of TiO_2 on a pilot-plant scale for purifying water [4–6]. Usually TiO_2 catalyst is utilized in the form of fine particle (i.e., suspensions of TiO_2 particles) or thin film (i.e., TiO_2 on robust substrates) in the photocatalytic systems. It is evident that the active surface area available for photoreactions is much larger in suspension systems than in film systems. But practical applications of this technique aim more at immobilizing TiO_2 catalysts onto various substrates since the separation of tiny TiO_2 particles from the purified water is inconvenient for suspension systems [7–12].

Up to now, improving the photocatalytic efficiency of TiO_2 thin-film photoreactors remains a major task in achieving maximum potential in commercial applications. Fortunately, this task can be fulfilled to a great extent by [11–18]: (1) using porous TiO_2 films to increase the active surface area for photoreactions; and (2) applying a positive potential bias on TiO_2 photocatalysts to suppress markedly the recombination rate of photogenerated electrons and holes. Under potential bias conditions, the photocatalytic reactions on TiO_2 surface may be considered as special electrode reactions involving electron-hole (*e-h*) pairs on TiO_2 photoelectrode/liquid interface. Thus, the photoelectrochemical degradation reactions of some model organic substances on TiO_2 electrodes were inspected in the literature through electrochemical tests, which provided useful information concerning photoreaction mechanism [17, 19], photoelectrocatalytic degradation kinetics [14, 15, 20], and even adsorption of organic compounds [21]. Obviously, potential bias is very important for photocatalytic technique of TiO_2, but there are very limited studies and principles to determine this parameter.

In this study, photoelectrochemical degradation behavior of various organic substances on nanoporous TiO_2 films was characterized with electrochemical impedance spectroscopy (EIS) and potentiodynamic polarization. Three compounds (i.e., formic acid, salicylic acid and methanol) were selected as the target organic contaminants in water on the basis of their different affinity to TiO_2 electrode surface and photo-

M. C. Li (✉) · J. N. Shen
Institute of Materials, Shanghai University, P.O. Box 269,
149 Yanchang Road, Shanghai,
200072 People Republic of China
E-mail: mouchengli@yahoo.com.cn

catalytic oxidation mechanism. Generally [22–24], (1) methanol is a well-known radical scavenger and a non-specific adsorbent to TiO_2 surface; (2) salicylic acid has strong surface interaction (i.e., chemisorption) with TiO_2 catalyst, and is oxidized directly by holes with byproducts adsorbed on TiO_2 surface; and (3) formic acid does not decompose through simple photolysis and electrolysis, but oxidizes to CO_2 through hole and/or hydroxyl radical, without producing stable intermediates. The main purposes of this work were to gain an insight into the photoelectrocatalytic oxidation characteristics of organic matters by TiO_2 catalysts, and to offer fundamental information for the application of positive potential bias in photocatalytic systems for water treatment.

Experimental

Test solutions

Sodium perchlorate ($NaClO_4 \cdot H_2O$), methanol, formic acid and salicylic acid with analytical grade were used. The supporting electrolyte was a 10 m mol/L (mM) $NaClO_4$ aqueous solution (i.e., base solution), which had very little effect on photocatalytic process of organic species [25]. Each test solution was prepared by dissolving one target organic compound in the base solution with a maximum concentration of 10 mM. Distilled water was used for preparing test solutions.

Preparation of TiO_2 films

Commercial titanium foils (purity > 99.7 wt.%) with dimensions of 60×10×0.2 mm were used to prepare TiO_2 films by anodization. The initial surface treatment was to grind with 800 grit waterproof abrasive paper and rinse with tap water. Prior to anodization, titanium plates were pickled in dilute HF solutions (5 vol.%) and cleaned with ethanol and distilled water. Titanium was anodized with a direct current power in 1 M H_2SO_4 solutions (ca. 25° C) at 100 V for 5 min to form TiO_2 films. The anodized films were characterized by field emission scanning electron microscopy (FESEM, JSM-6700F) and X-ray diffraction (XRD, Rigaku D/max 2550V) with Cu Kα radiation.

Electrochemical tests

Each electrochemical experiment was performed at room temperature in a three-electrode system which was established on a beaker containing 100 mL test solution without pH control and any aeration. A saturated calomel electrode (SCE) and a platinum foil served as the reference electrode and counter electrode, respectively. TiO_2 film was bent to immerse horizontally an area of 1 cm^2 into test solution and 2 mm lower than the solution surface, which was used as working electrodes. As an illuminant, a 40 W high pressure mercury lamp was located about 6 cm above the solution surface. All experiments were carried out in these cases in order to keep the intensity of incident ultraviolet (UV) light constant.

Measurements by EIS were conducted using an electrochemical measurement system from PAR (Princeton Application Research, AMETEK Inc.), which comprised an M273A potentiostat, an M5210 lock-in amplifier and the PowerSine software. An alternating current signal with the frequency range from 98 kHz to 10 mHz and an amplitude of 10 mV (rms) was applied to the working electrode at the open circuit potential (OCP). EIS spectra were interpreted using the non-linear least square (NLLS) fitting procedure developed by Boukamp [26]. Values of OCP and polarization curves were obtained with an electrochemical measurement system, which included an M273A and the M352 software. Potentiodynamic polarization curves were determined with a potential scan rate of 2 mV/s, which could be a type of quasi-steady state measurement. All experiments were repeated by using different specimens to confirm reproducibility of the results.

Results and discussion

Characteristics of TiO_2 films

After titanium foils were anodized in H_2SO_4 solution at 100 V, the surfaces became porous as shown in Fig. 1. The size of pores is less than 150 nm. Apparently the anodized foils were covered by oxide films in which only TiO_2 with anatase structure was detected by XRD (not shown), as widely described in the literature [17, 27, 28]. It was known that TiO_2 photocatalysts in anatase phase had much higher photocatalytic properties than in other phases [29]. The films formed in this case are about

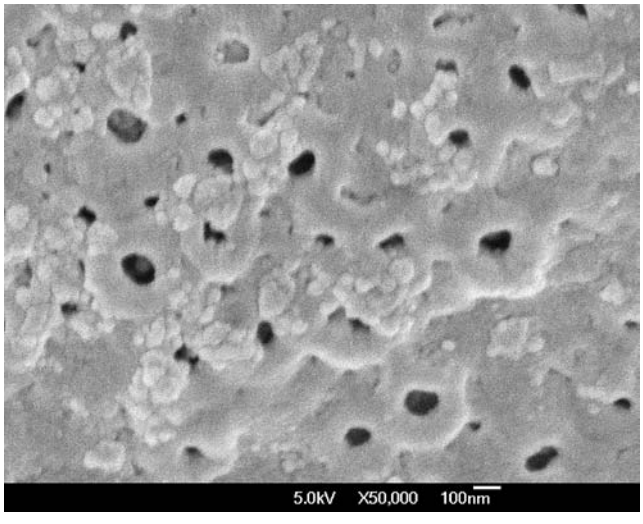

Fig. 1 FESEM morphologies of anodic TiO_2 films formed at 100 V in H_2SO_4 solution

240 nm in thickness, simply assumed a growth constant of 2.42 nm/V and an initial film thickness of about 1 nm [30]. Obviously, TiO_2 thin-films prepared by anodization should have not only good adhesion to titanium substrate but also coarse surfaces for photoelectrocatalytic reactions because the films were directly grown from titanium substrate and had nanoporous surface structure, which cannot be obtained through other film-forming techniques such as sol-gel methods and thermal oxidation [8, 31, 32].

Figure 2 gives the typical Bode plots of EIS spectra for TiO_2 film in the test solutions under dark condition. Some points at initial high-frequency part were omitted because of the appearance of high-frequency phase shift [33]. Experimental data were also compared with the fitted values obtained from data processing as described later. The lines represent the model calculations. It can be seen that log|Z| is linear with log f and phase angle θ has values close to 80° in the low frequencies ($f < 0.1$ Hz). These are characteristics of a predominantly capacitive behavior [34, 35], indicating that titanium substrate/TiO_2 film electrode systems were in passive state in the solutions. Furthermore, polarization curves showed that the values of passive current density were less than 1 μA/cm^2 in all test solutions under dark conditions with increasing the applied potentials to 1.2 V versus OCP (not shown here). Thus, the titanium substrates were assumed to be separated from solutions by TiO_2 thin-films, which implied that the photoelectrochemical performance of TiO_2 films could be measured with insignificant influence of titanium substrate.

Variation of OCP

Figure 3 shows OCP versus UV-illumination time curves for anodic TiO_2 films in various solutions. As soon as the TiO_2 electrodes were illuminated with UV light, all OCP dropped down to much more negative values as a result of the sudden creation of *e-h* pairs in the films [36, 37]. Owing to the balancing rate between creation and depletion of photogenerated carriers, each OCP tended to stabilize after several minutes of irradiation. The approximately unchanging OCP values meant that steady states of photoreactions were attained on TiO_2 film electrodes. As compared with in the base solution, the relatively stable OCP shifted to lower values in formic acid or methanol solutions, and to higher values in salicylic acid solutions. In general, the presence of organic species is able to consume holes and let more electrons accumulate in TiO_2 film, which reduced OCP values. With the same concentrations, formic acid showed higher activity in lowering OCP than methanol. The increase of OCP with adding salicylic acid into the base solutions might be explained by the strong chemisorption of byproducts on TiO_2 electrode surface [22, 23, 38].

EIS spectra at OCP

Because photoelectrochemical oxidation reactions are caused by the photogenerated *e-h* pairs on TiO_2 electrode surface, EIS technique can be used as a very fast and in-situ method for evaluating the oxidation process of organic species at OCP [19, 20]. Certainly, it cannot detect the photochemical oxidation that has taken place in the solution instead of on the electrode surface. Figure 4 shows Nyquist plots for the TiO_2 photoelectrode in the three types of organic solutions at OCP. Each EIS spectrum only shows one capacitive arc in the Nyquist plot and one peak in the Bode plot (not shown), suggesting that charge transfer was the control step for photoelectrocatalytic oxidation reactions of the species

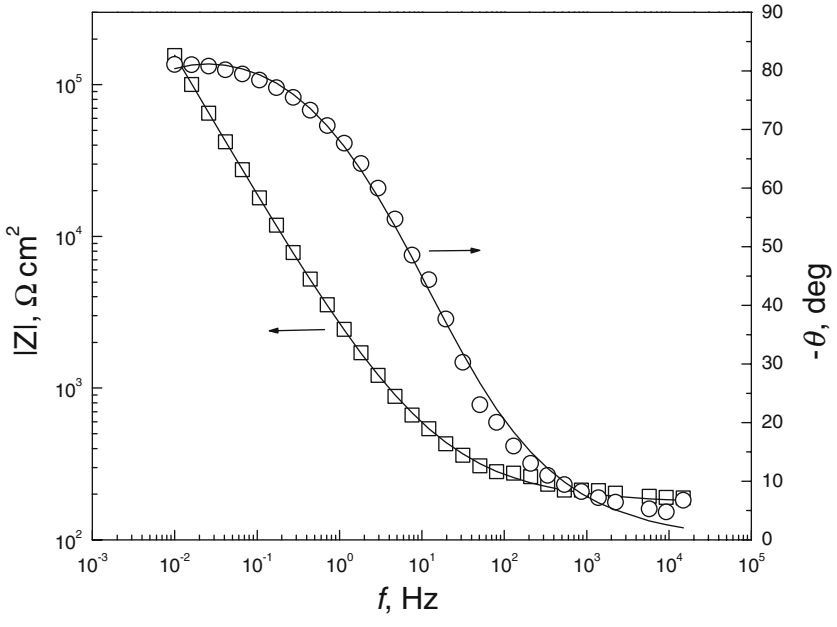

Fig. 2 Bode plots for TiO_2 film in 1 mM formic acid solution without UV illumination. *Symbols* experimental data; *lines* fitted values

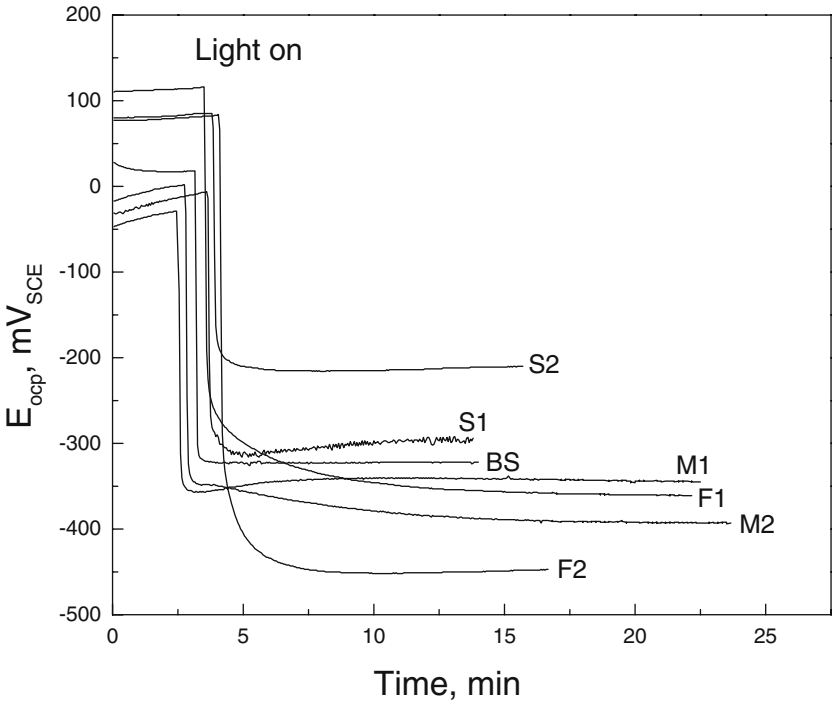

Fig. 3 Variation of open circuit potential with time for TiO_2 film electrodes in different solutions under UV illumination. *BS* base solution; S1 and S2, 0.1 and 0.5 mM salicylic acid solutions; M1 and M2, 1 and 10 mM methanol solutions; F1 and F2, 1 and 10 mM formic acid solutions

[20]. The oxidation mechanism did not change with increasing the concentration of organic species. Thus, the electrode potential would be the controlling parameter of the electrode kinetic reactions under present UV light. Furthermore, TiO_2 electrodes showed similar impedance values (i.e., the size of the arc radius) in all solutions except in 10 mM formic acid solution. Particularly, owing to the strong affinity of salicylic acid, the TiO_2 electrode surface might reach a saturated adsorption at 0.1 mM. The increase of its concentration up to 0.5 mM had no influence on impedance size because only the molecules in direct contact with the surface underwent photooxidation. These results imply that the photoelectrocatalytic degradation rate of these organic species had no significant difference at OCP and was dominated by the generation and separation of *e-h* pairs.

Though the time constant from TiO_2 film itself was very difficult to be defined, the equivalent circuit [37, 39] in Fig. 5 was proposed as a model for the electrochemical system TiO_2 film/solution under both dark and illumination conditions, due to the existence of thin TiO_2 films on the titanium substrates. R_s represents the electrolyte resistance, R_f and C_f represent the resistance and capacitance of TiO_2 film, R_t and C_{dl} represent the charge transfer resistance and double layer capacitance, respectively. In addition, both C_f and C_{dl} were replaced with constant phase element (CPE) in the fitting procedure due to the non-ideal capacitive response of the interface TiO_2 film/solution. The impedance of CPE is given by [40]

$$Z_{CPE} = \frac{1}{Y_0(j\omega)^{\alpha}} \quad (1)$$

where Y_0 is the admittance magnitude of CPE, and α is the exponential term. Pure capacitance behavior is represented by $\alpha = 1$. In practice, α is in the range zero to one.

The model fitted the experimental data very well in spite of the approximations made, as shown in Figs. 2 and 4. It can be concluded that the model provided a reliable description for the electrochemical systems. Table 1 gives the fitted results of EIS spectra for TiO_2 films in the solutions with different concentrations of formic acid in the absence and presence of UV light. The relative errors from the fitting can reach 70% for R_t in the dark because of the poor definition of the trend of EIS in the low frequencies, and are less than 5% for other parameters.

The value of R_t in the dark is of the order of $10^6 \Omega\ cm^2$, due to the passive state of titanium/TiO_2 film electrodes in test solutions [37]. For a simple comparison, the values of R_f and R_t under UV illumination are significantly smaller than those in the dark, respectively. From dark to illumination, the photoeffect in TiO_2 films results in the huge changes of R_f [41], while the appearance of oxidation of water (H_2O) and formic acid as anodic reaction on TiO_2 films reduces R_t by a factor of 700 or more. Moreover, about one half of R_t was reduced as a result of increasing formic acid concentration from 1 to 10 mM, indicating that more *e-h* pairs were separated by formic acid, and then more holes were available to oxidize H_2O and formic acid [11].

Potentiodynamic polarization curves

Figure 6 shows anodic polarization curves for the TiO_2 photoelectrode in base solution and different organic

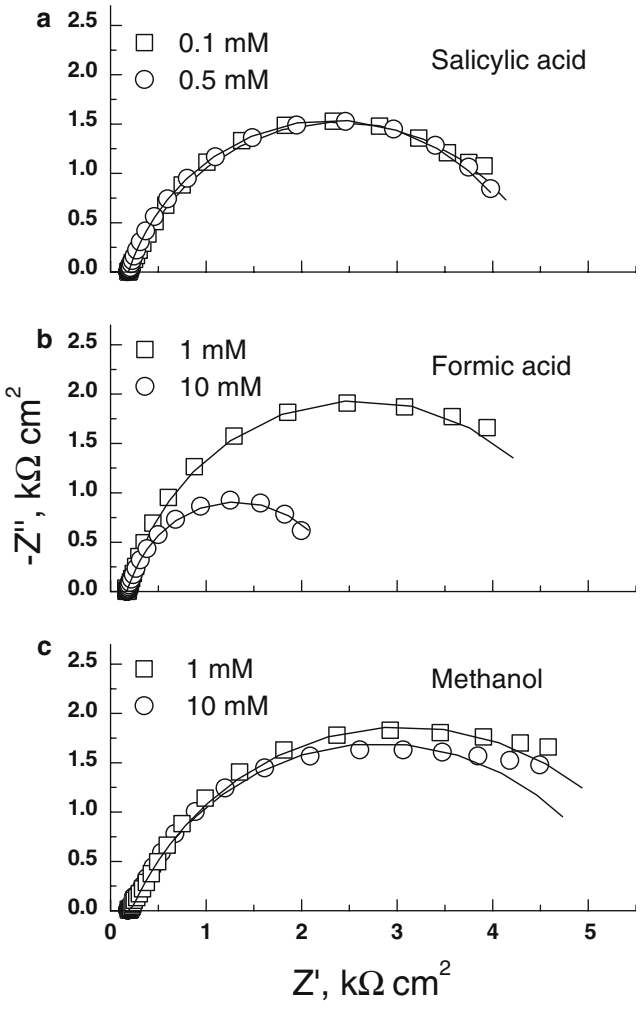

Fig. 4 Nyquist plots for TiO_2 film electrodes in different solutions under illumination. *Symbols* experimental data; *lines* fitted values

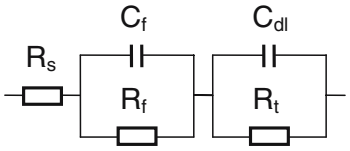

Fig. 5 Equivalent circuit of the electrochemical system TiO_2 film/solution. R_s, electrolyte resistance; R_f and C_f, resistance and capacitance of TiO_2 film; R_t, transfer resistance; C_{dl}, double layer capacitance

solutions, where ΔE (applied potential bias or applied voltage) is equal to the electrode potential difference between applied potential (E) and OCP, namely

$$\Delta E = E - E_{ocp} \quad (2)$$

In the literature [11, 22, 23], the effect of potential bias was often estimated by the values of photocurrent density (i_{ph}) at a given electrode potential in E versus i_{ph} curves. But in fact, polarized degrees (i.e. ΔE values) were different at a given potential for organic species with various concentrations, due to the different OCP values as shown in Fig. 3. Thus, E versus i_{ph} curve was inconvenient for this purpose, and ΔE versus i_{ph} curves were adopted in Fig. 6.

As far as the base solution is concerned in Fig. 6, three parts of i_{ph} can be discerned with the increase of ΔE. At the initial bias potentials within ca. 0.26 V, i_{ph} increases slowly and non-linearly, being indicative of the low separation rates for photogenerated *e-h* pairs under the low electric field intensity conditions over the TiO_2 photoelectrode system. At higher bias potentials, i_{ph} is characterized by the linear change. It is assumed that the electron transport in TiO_2 film becomes the rate-limiting step, and then the TiO_2 photoelectrode behaves as a constant resistance rather than a variable resistance [42, 43]. With further increasing bias potential, i_{ph} levels off and tends to stabilize. This behavior is called as saturation, which mainly results from scanty holes to facilitate the interface reactions and is related to light intensity [21, 42].

As can be seen, the characteristics of i_{ph} in organic solutions are similar to those in the base solution. In the base solution, only H_2O was oxidized at TiO_2 electrode surface by the photogenerated holes, while both H_2O and organic species were oxidized in organic solutions. Except salicylic acid solutions, the addition of organic species into the base solution results in the increase of i_{ph} at all the tested bias potentials, and the higher concentrations of organic species the larger i_{ph}. These may be caused by the competitive oxidation of organic species with H_2O and the current doubling effect of the free radicals formed by subsequent photoreactions of organic species [11, 44]. The organic species might have little influence on photooxidation of H_2O due to their very low concentrations [21]. Therefore, the photooxidation rate (Δi_{ph}) of pure organic species is approxi-

Table 1 Fitted results of EIS spectra for TiO_2 film electrodes in formic acid solutions

R_s /Ω cm^2	$Y_{0\text{-}f}$ /s$^\alpha$ Ω cm^{-2}	α_f	R_f /Ω cm^2	$Y_{0\text{-}dl}$ /s$^\alpha$ Ω cm^{-2}	α_{dl}	R_t /Ω cm^2
In 0.01 M $NaClO_4$ + 0.001 M formic acid solution in the dark						
185	4.43×10^{-4}	0.48	1813	8.33×10^{-5}	0.93	3.38×0^6
In 0.01 M $NaClO_4$ + 0.001 M formic acid solution under illumination						
174	4.90×10^{-3}	0.83	26	8.31×10^{-4}	0.86	4840
In 0.01 M $NaClO_4$ + 0.01M formic acid solution under illumination						
172	5.96×10^{-3}	0.94	23	1.79×10^{-3}	0.87	2240

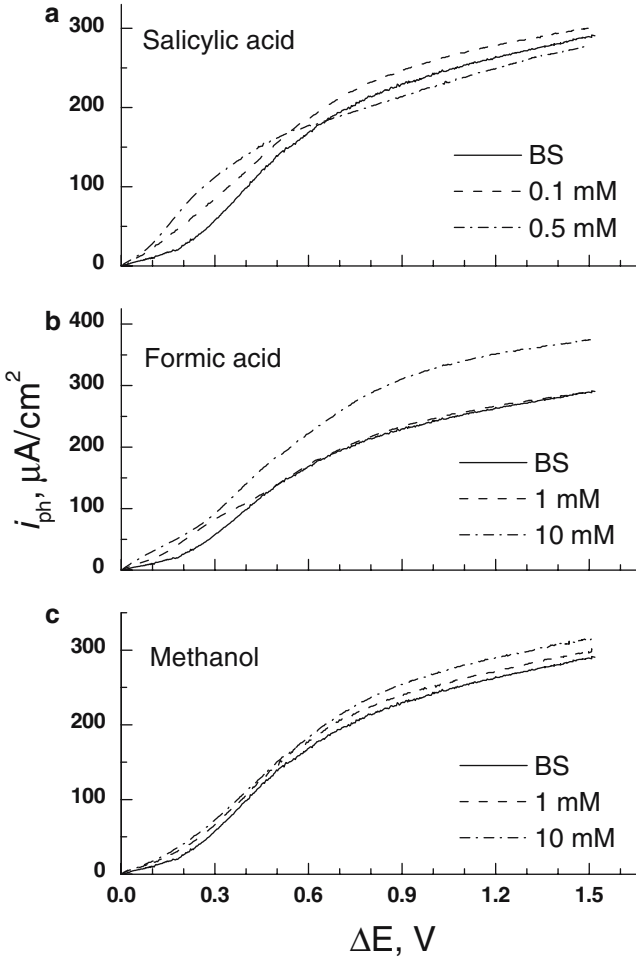

Fig. 6 Polarization curves for TiO_2 film electrodes in different organic solutions under UV light

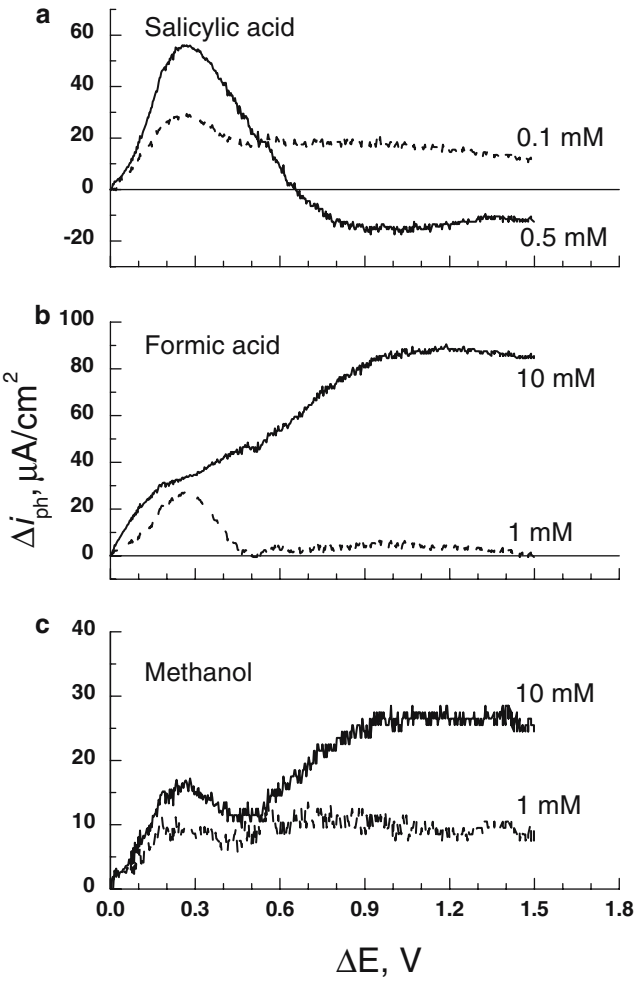

Fig. 7 Variations of photooxidation current density for pure organic substances with potential bias on TiO_2 films

mately equal to the difference of i_{ph} between the organic solution and base solution, obtained by

$$\Delta i_{ph} = (i_{ph})_{organic} - (i_{ph})_{base}. \quad (3)$$

Figure 7 gives the plots of Δi_{ph} versus ΔE. One peak of the photooxidation rate appears at ca. 0.26 V and the higher concentrations of organic species the larger peak rates. As discussed above, in low potential bias range, photogenerated *e-h* pairs had a low separation rate in the base solution. When organic species were present, they not only had the current doubling effect but also could reduce the *e-h* recombination rate. The photooxidation peak may represent a result of these two effects, and the more organic species adsorbed on TiO_2 electrode surface the more these effects which can be confirmed further by the peak values in different organic solutions. Compared with formic acid, salicylic acid shows a higher peak due to its strong affinity to TiO_2 surface, while methanol shows a lower peak due to its weak affinity. After this peak, the separation rate of *e-h* pairs cannot be affected by organic species. The linear increase in photooxidation rate of H_2O may lead to the decrease in photooxidation rates of organic species with the lower concentrations. After ca. 0.6 V, the photooxidation rates of salicylic acid (0.1 mM), formic acid (1 mM) and methanol (1 mM) are almost constant and far less than that of H_2O. When the concentrations of formic acid and methanol change to 10 mM, their photooxidation rates increase with potential bias and reach stability at ca. 1 V. This is because the more organic species can adsorb on TiO_2 surface under the higher concentration conditions. But, the photooxidation rate of salicylic acid (0.5 mM) decreases to negative values, indicating that the photooxidation rate of 0.5 mM salicylic acid solution is lower than that of the base solution after ca. 0.66 V, as shown in Fig. 6(a). The main reason is that the byproducts adsorbed on the TiO_2 electrode surface may inhibit the photoreactions of H_2O and salicylic acid [22, 23, 38].

Obviously, the photooxidation rate curves of organic species instead of their organic solutions should be more suitable for optimizing the potential bias values in photoelectrocatalytic oxidation systems. In the very low concentration cases, the potential bias at the rate peak is the optimum value, while both the stable photooxida-

tion rate and faradaic efficiency are going to be considered in the higher concentration cases.

Conclusions

TiO_2 thin-films with nanoporous surface and anatase phase were prepared by anodization of titanium foils in sulfuric acid solutions. From dark to ultraviolet illumination, OCP and film resistance of TiO_2 films decreased markedly. The photoelectrocatalytic oxidation process of salicylic acid, formic acid and methanol on TiO_2 films had similar EIS characteristics at OCP. The simple photoreactions were controlled by the charge transfer step. Values of the charge transfer resistance could be used to evaluate the overall rate of photoreactions.

According to the potentiodynamic polarization curves of the base solution and organic solutions, the kinetic rate curves for the photoelectrocatalytic oxidation of pure organic species could be obtained as a function of the potential bias. The photooxidation rates changed with organic concentrations—for formic acid and methanol from 1 to 10 mM, their photooxidaiton rates increased, while for salicylic acid from 0.1 to 0.5 mM, its photooxidation rate decreased after 0.66 V, even lower than the photooxidation rate of water. One oxidation peak at a bias potential of ca. 0.26 V was observed for these species, and the higher concentrations of organic species within present concentration ranges the larger peak values. After the potential bias increased to ca. 1 V, the photooxidation rate reached stable values, and the photooxidation rate of water was much larger than that of organic species.

Acknowledgements This work was supported by the Natural Science Foundation of China (NSFC) and Shanghai BaoSteel Company (Grant No. 50471105), Shanghai Science & Technology Council (0352nm074), and Shanghai Municipal Education Commission (04AE96).

References

1. Fujishima A, Rao TN, Tryk DA (2000) J Photochem Photobiol C: Photochem Rev 1:1
2. Mills A, Hunte SL (1997) J Photochem Photobiol A: Chem 108:1
3. Dominguez C, Garcia J, Pedraz MA, Torres A, Galan MA (1998) Catal Today 40:85
4. Malato S, Blanco J, Vidal A, Richter C (2002) Appl Catal B: Environ 37:1
5. Goslich R, Dillert R, Bahnemann D (1997) Wat Sci Tech 35:137
6. Feitz AJ, Boyden BH, Waite TD (2000) Wat Res 36:3927
7. Lin WY, Tacconi NR, Smith RL, Rajeshwar K (1997) J Electrochem Soc 144:497
8. Byrne JA, Eggins BR, Brown NMD, McKinney B, Rouse M (1998) Appl Catal B: Environ 17:25
9. Dijkstra MFJ, Buwalda H, Jong AWF, Michorius A, Winkelman JGM, Beenackers AACM (2001) Chem Eng Sci 56:547
10. Chan AHC, Chan CK, Barford JP, Porter JF (2003) Wat Res 37:1125
11. Candal RJ, Zeltner WA, Anderson MA (2000) Environ Sci Technol 34:3443
12. Butterfield IM, Christensen PA, Hamnett A, Shaw KE, Walker GM, Walker SA (1997) J Appl Electrochem 27:385
13. Kim DH, Anderson MA (1994) Environ Sci Technol 28:479
14. Vinodgopal K, Stafford U, Gray KA, Kamat PV (1994) J Phys Chem 98:6797
15. Byrne JA, Eggins BR (1998) J Electroanal Chem 457:61
16. Zhang W, An T, Xiao X, Fu J, Sheng G, Cui M, Li G (2003) Appl Catal A: Gen 255:221
17. Li XZ, Li FB (2002) J Appl Electrochem 32:203
18. Leng W, Liu H, Cheng S, Zhang J, Cao C (2000) J Photochem Photobiol A: Chem 131:125
19. Liu H, Li XZ, Leng YJ, Li WZ (2003) J Phys Chem B 107:8988
20. Liu H, Cheng S, Wu M, Wu H, Zhang J, Li W, Cao C (2000) J Phys Chem A 104:7016
21. Jiang D, Zhao H, Zhang S, John R, Will GD (2003) J Photochem Photobiol A: Chem 156:201
22. Calvo ME, Candal RJ, Bilmes SA (2001) Environ Sci Technol 35:4132
23. Mandelbaum P, Bilmes SA, Regazzoni AE, Blesa MA (1999) Solar Energy 65:75
24. Selcuk H, Zaltner W, Sene JJ, Bekbolet M, Anderson MA (2004) J Appl Electrochem 34:653
25. Abdullah M, Low GKC, Matthews RW (1990) J Phys Chem 94:6820
26. B.A. Boukamp (Oct. 1989) Proceedings of the ninth European Corros Cong, EFC, Vol. 1, Paper No. FU-252, Utrecht, The Netherlands
27. Birch JR, Burleigh TD (2000) Corrosion 56:1233
28. Arsov LD, Kormann C, Plieth W (1991) J Electrochem Soc 138:2964
29. Sclafani A, Herrmann JM (1996) J Phys Chem 100:13655
30. Sul YT, Johansson CB, Jeong Y, Albrektsson T (2001) Med Eng Phys 23:329
31. Hattori A, Tokihisa Y, Tada H, Tohge N, Ito S, Hongo K, Shiratsuchi R, Nogami G (2001) J Sol-Gel Sci Technol 22:53
32. Leng WH, Zhang Z, Zhang JQ (2003) J Mol Catal A: Chem 206:239
33. Li MC, Zeng CL, Lin HC, Cao CN (2001) Bull Electrochem 17:299
34. Burleigh TD, Smith AT (1991) J Electrochem Soc 138:L34
35. Li MC, Luo SZ, Zeng CL, Shen JN, Lin HC, Cao CN (2004) Corros Sci 46:1369
36. Byrne JA, Davidson A, Dunlop PSM, Eggins BR (2002) J Photochem Photobiol A: Chem 148:365
37. Li MC, Luo SZ, Wu PF, Shen JN (2005) Electrochim Acta 50:3401
38. Kratochvilova K, Hoskovcova I, Jirkovsky J, Llima J, Ludvik J (1995) Electrochim Acta 40:2603
39. Vanmaekelbergh D (1997) Electrochim Acta 42:1121
40. Wu X, Ma H, Chen S, Xu Z, Sui A (1999) J Electrochem Soc 146:1847
41. Eppler AM, Ballard IM, Nelson J (2002) Phys E 14:197
42. Jiang D, Zhao H, Jia Z, Cao J, John R (2001) J Photochem Photobiol A: Chem 144:197
43. Jiang D, Zhao H, Zhang S, John R (2003) J Phys Chem B 107:12774
44. Freund T, Gomes WP (1969) Catal Rev 3:1